Caving 2010 — Y. Potvin (ed)
© 2010 Australian Centre for Geomechanics, Perth, ISBN 978-0-9806154-1-8
doi:10.36487/ACG_rep/1002_11_Sainsbury

Investigation of caving induced subsidence at the abandoned Grace Mine

D.P. Sainsbury *Itasca Australia Pty Ltd, Australia*

B.L. Sainsbury *Itasca Australia Pty Ltd, Australia*

L.J. Lorig *Itasca Consulting Group, Inc., United States of America*

Abstract

The Grace Mine, located in southeast Pennsylvania USA, was owned and operated by Bethlehem Steel Corporation from 1951–1977. During this time, iron ore was extracted using the underground panel caving mining method that has resulted in significant surface subsidence. Upon recovery of the water table after mining, a lake has formed over much of the subsided area. Prior to redevelopment of the abandoned mine site for residential and light industrial usage, investigation of the subsidence zone of influence, and the potential for further subsidence has been undertaken.

1 Introduction

During 1951–1977, approximately 33 million tonnes of iron ore was extracted using the panel caving mining method. Due to the close proximity (approximately 80 km) to Philadelphia, the sixth most populous city in the United States, the abandoned mine site offers much needed land for residential and light industrial usage. Prior to redevelopment of the abandoned mine site, a thorough understanding of the extents of caving-induced subsidence and the potential for future subsidence is required.

The time associated with subsidence resulting from mining is composed of two distinct phases: active and residual. Active subsidence refers to all movements occurring simultaneously with the mining operations; residual subsidence is that part of the surface deformation that occurs following the cessation of mining. The duration of residual subsidence is of particular importance from the standpoint of evaluating the extent of liability of underground mine operators and developers for post-mining subsidence and land use.

2 History of Grace Mine

Iron ore mining began in southeastern Pennsylvania before the American Revolutionary War (1775–1783) and reached the peak of activity during the 1880s. In 1948, airborne magnetometer surveying conducted by the Bethlehem Steel Corporation led to the discovery of a large, deep magnetite deposit located approximately 3.2 km north of Morgantown, in Berks County, southeast Pennsylvania. Diamond drilling from 1949–1951 delineated the orebody, which was named the Grace Mine.

Development of the Grace Mine commenced in 1951 with construction of two vertical shafts to gain access to the orebody. Shaft A was developed to a depth of 784 m, and Shaft B was developed to a depth of 938 m with a diameter of 5.3 m. The plant area, located near the shaft collars, included an office and change house, hoist house, warehouse and repair shop, milling and pelletising buildings, and extensive railroad facilities (illustrated in Figure 1). The two shafts and all surface infrastructure were constructed outside an area formed by a conservative 45° subsidence angle (measured from the base of the underground workings). None of the existing Grace Mine buildings have shown signs of subsidence-induced damage to date.

The Grace Mine orebody contained an estimated 107 million t of magnetite averaging 40% iron ore. During the active mining period between 1958–1977, approximately 33 million t of ore were mined primarily with the inclined panel caving method (Eben, 2004, written comm.). Initial development of the Grace Mine orebody was conducted using slushing drifts (or scrapers) to scoop the ore into underground rail cars. From 1966–1969, the mine was converted to a mobile mining system, replacing slushing drifts and an electric rail system with diesel-powered load–haul–dump (LHD) vehicles. The main production drives were developed at dimensions of 4 × 4.5 m.

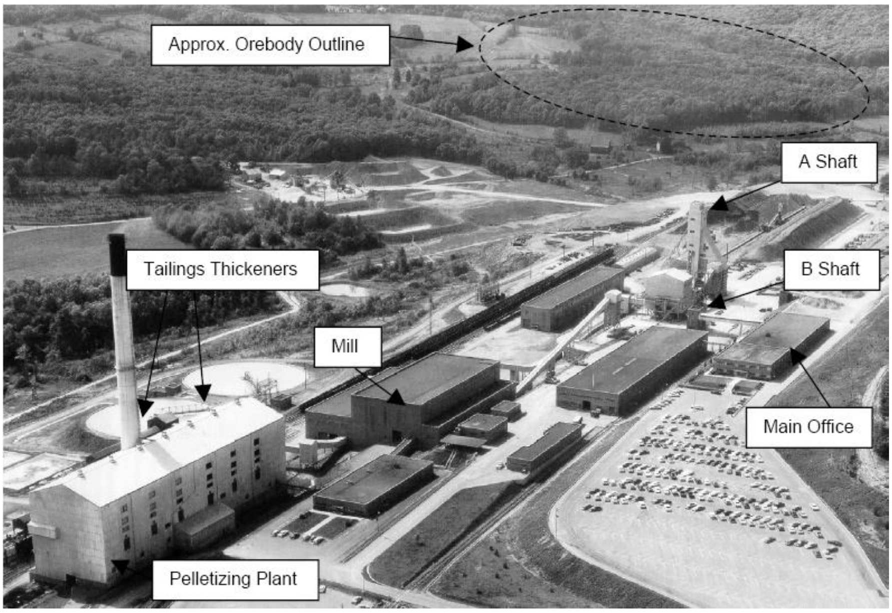

Figure 1 Surface infrastructure at the Grace Mine, looking northeast, early 1960s

Figure 2(a) illustrates the extent of the underground development at Grace Mine together with the approximate undercut outline. Figure 2(b) illustrates a schematic of the inclined panel caving method employed at the Grace Mine.

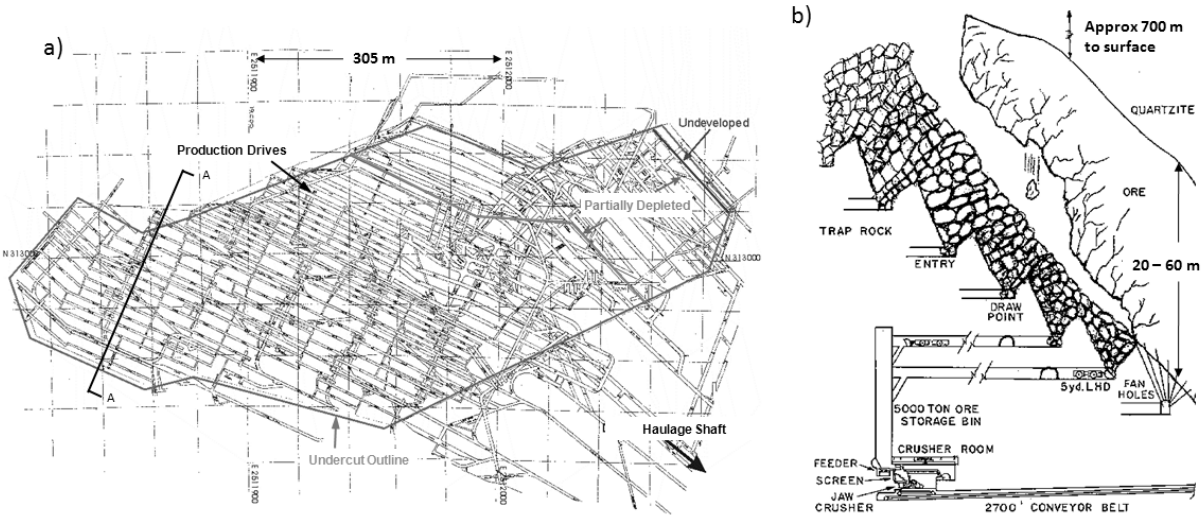

Figure 2 a) Extent of underground production drives (plan view); and b) two-dimensional schematic of panel caving at Grace Mine (after Stafford, 2002)

Mining operations ceased in 1977 due to an influx in foreign steel imports, increased costs of environmental regulation and increased costs of underground mining. At the completion of mining, mining-induced subsidence had significantly altered the topography above the mine workings. Mine dewatering continued until 1981 (Stafford, 2002). Upon recovery of the water table, a lake formed over the subsided area, as illustrated in Figure 3.

Figure 3 Present day subsidence lake

3 Characteristics of caving induced subsidence

A review of large-scale surface disturbances from block and panel caving mines was conducted by Lupo (1999), who found that the primary surface features that develop as a result of block and panel caving include one or more of the following zones:

- a caved rock zone
- a large-scale surface cracking (fractured) zone
- a small-scale surface displacement (continuous surface subsidence) zone
- a stable zone.

In addition, chimney caving was found to be a prominent secondary surface disturbance feature. Figure 4 illustrates the terminology used to describe subsidence features related to block and panel caving. Historically, mining engineers have defined the extent of subsidence features using angles measured from the base of the undercut. However, caution should be used when using such quoted angles to predict subsidence, because factors such as the mining depth and rock mass properties have a significant effect on the angles of break and subsidence. The use of angles measured from the base of the workings implies that the failure mechanism develops along a plane, although the actual failure surface may take any shape in situ.

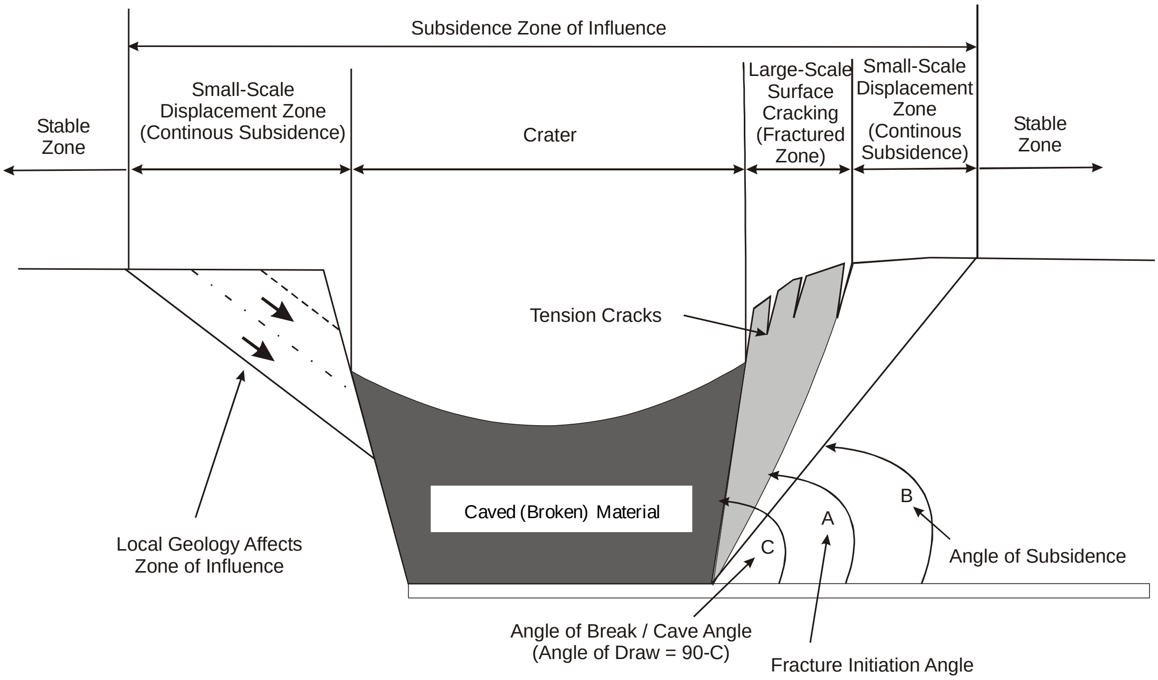

Figure 4 Terminology used to describe subsidence features

4 Geomechanical properties of the Grace Mine rock units

Currently, the only drill core information available from the Grace Mine site are drilling logs from a diamond drilling program conducted during 1998 to investigate the near-surface conditions (< 30 m) for construction of a large-scale industrial facility near the western edge of the subsidence lake. Due to the location of the drill holes above the mining horizon, the intersected rock mass has been disturbed by the caving process and does not represent the in situ (pre-mining) rock mass condition.

The following descriptions of the rock units at the Grace Mine have been compiled from the aforementioned drilling logs, mapping of surface outcrops and other available literature.

4.1 Regional geology

Sedimentary rocks of Triassic age occupy a series of trough-like isolated basins that occur from Nova Scotia to South Carolina. The largest basin, commonly known as the Newark Basin, extends from New York City to northern Maryland. Basaltic magma intruded the basin toward the end of the Triassic period, forming thick intrusive diabase sheets.

4.2 Local geology

Three rock types are associated with the Grace Mine: diabase footwall; replaced limestone; and Triassic sediments. Sims (1968) suggests that the magnetite deposit occurs in a lens of Cambrian limestone that is overlain unconformably by Triassic sedimentary rocks. The magnetite deposit was formed by replacement of contact metamorphic minerals in the limestone lens, caused by the intrusion of an underlying diabase sheet. The orebody is roughly tabular in shape, strikes approximately 60° and dips 20–30° to the northeast. It is approximately 1,067 m long × 213–457 m wide, and ranges from less than 15 m to more than 121 m in thickness. Figure 5(a) illustrates an isometric view of the original ground surface and orebody shape. The surfaces were reconstructed from the original mine geological cross-sections (Eben, 2004, written comm.).

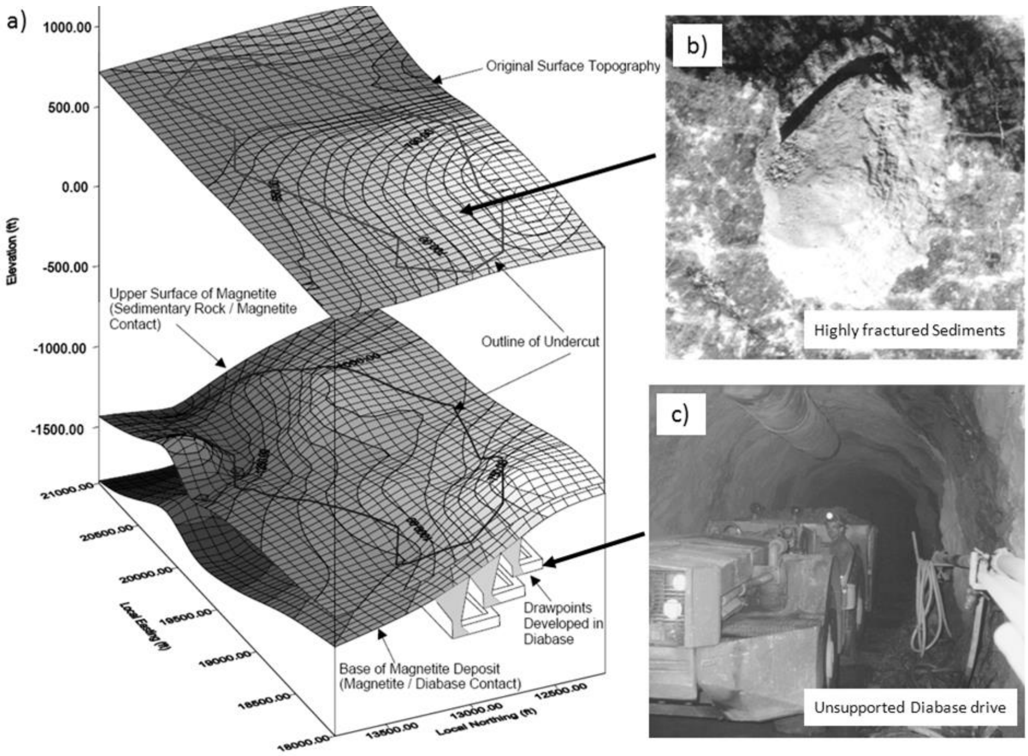

Figure 5 Isometric view of original ground surface and orebody limits

Of interest to the investigation of mining-induced subsidence is the nature of the sedimentary rocks that overlie the orebody. Sims (1968) and Basu (1974) identify the Triassic sedimentary rocks that form the hangingwall of the ore deposit as the Stockton Formation. The formation consists of inter-bedded sandstone, shale and conglomerate. The Stockton Formation is overlain by the Brunswick Formation, which also consists of poorly sorted inter-fingered sandstone, shale and conglomerate layers. The top of the Brunswick Formation has been eroded to form the ground surface directly above the orebody. Surface outcrops of the Stockton Formation near the Grace Mine are thinly bedded and highly fractured, with very closely spaced (<100 mm) vertical and open joints. The conglomerate layers of the Stockton Formation are thickly bedded (0.5–1.5 m) and moderately fractured (0.5–2 m), with vertical and open joints.

4.3 Geomechanical properties of main rock types

The properties used to represent the different rock masses at the Grace Mine site are listed in Table 1.

Table 1 Material properties used to estimate Grace Mine rock mass strength

Material	GSI	UCS (MPa)	m_i
Sediments (upper bound)	55	100	12
Sediments (best estimate)	45	60	12
Sediments (lower bound)	30	40	12
Limestone	55	90	15
Magnetite (ore)	45	40	9
Diabase (footwall)	60	200	25

Geological Strength Index (GSI); Unconfined compressive strength (UCS)

4.4 Pre-mining stress regime

The pre-mining stress was measured directly at Grace Mine using the United States Bureau of Mines (USBM) Deformation Gage Technique. Agarwal et al. (1973) detail the measurement procedure for 36 deformation measurements from three separate boreholes. The boreholes were located to ensure that the measured stress regime was representative of the pre-mining stress regime (unaffected by nearby excavations).

The stress regime presented in Table 2 is an average of measurements made at a depth of 731 m below the ground surface.

Table 2 Pre-mining stress regime at 731 m below surface

Principal Stress	Magnitude (MPa)	Dip (°)	Azimuth (°)
Sigma 1	51.5	16	027
Sigma 2	29.0	22	103
Sigma 3	26.2	85	181

5 Caving-induced subsidence at the Grace Mine

5.1 Evolution of subsidence crater and trough

From 1959–1969, engineers from the USBM monitored the evolution of surface subsidence at the Grace Mine. No USBM Report of Investigation was published on the extensive subsidence monitoring program. However, during the course of this investigation, several hand written memorandums from USBM Engineers to management of the Grace Mine were recovered from former Grace Mine superintendent, Mr Charles Taylor's private collection. Goodman (1970) reported the evolution of the subsidence trough as follows:

10 December 1962 — First indication that subsidence was beginning.

18 February 1963 — Cracks on the surface were noted, and a slumped zone widened and steadily descended.

16 December 1963 — The underground caved to the surface.

17 April 1964 — Cracks extended to circle the crater and extended in a concentric pattern.

8 June 1965 — The subsidence trough was observed to progress to the northeast.

3 June 1969 — The subsidence trough moves to the northeast following the development and extraction pattern.

Figure 6 illustrates different aerial views of the subsidence trough. The initial cave breakthrough appears to have been facilitated by the presence of a steeply dipping joint/fault structure oriented at approximately 60°. As the subsidence trough progressed to the northeast, the actual cave did not break through to the surface. In the southwestern section of the subsidence trough, large concentric surface cracks can be observed, while two sets of cracks oriented at approximately 60° and 110° are observed in the northeastern section. The ground within the approximate extent of surface cracking can be clearly observed to be highly fractured and disturbed.

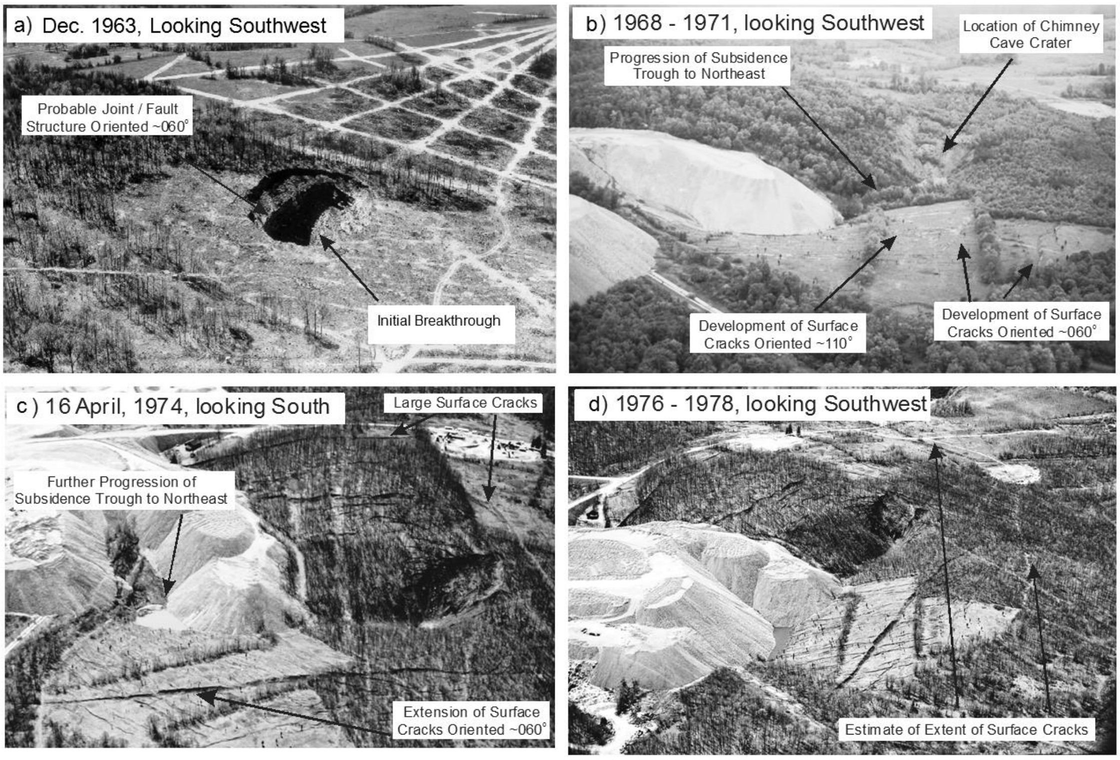

Figure 6 Evolution of subsidence from 1963–1978

Approximately 30 monuments were installed on the surface above the mining horizon and monitored by the USBM between 1962–1969. Surveying techniques used over the monitoring period included chaining, levelling and triangulation. The maximum elevation change as of 1969 was reported to be 35 m. Goodman (1970) noted that uplift generally occurred in pins around the periphery of the orebody outline, while acceleration of subsidence was greatest directly over recently developed panels. Surface uplift outside the undercut footprint was also monitored at the Lakeshore Mine in Arizona (Panek, 1984).

5.2 Visual observation of the limit of large-scale surface cracking

Figure 7 illustrates the results of a field survey conducted during June 2004 to identify the extent of large-scale surface cracking surrounding the subsidence trough. The furthest observable surface cracks from the orebody outline have been mapped and used to generate a contour line that represents the limit of the large-scale surface cracking zone (fractured zone).

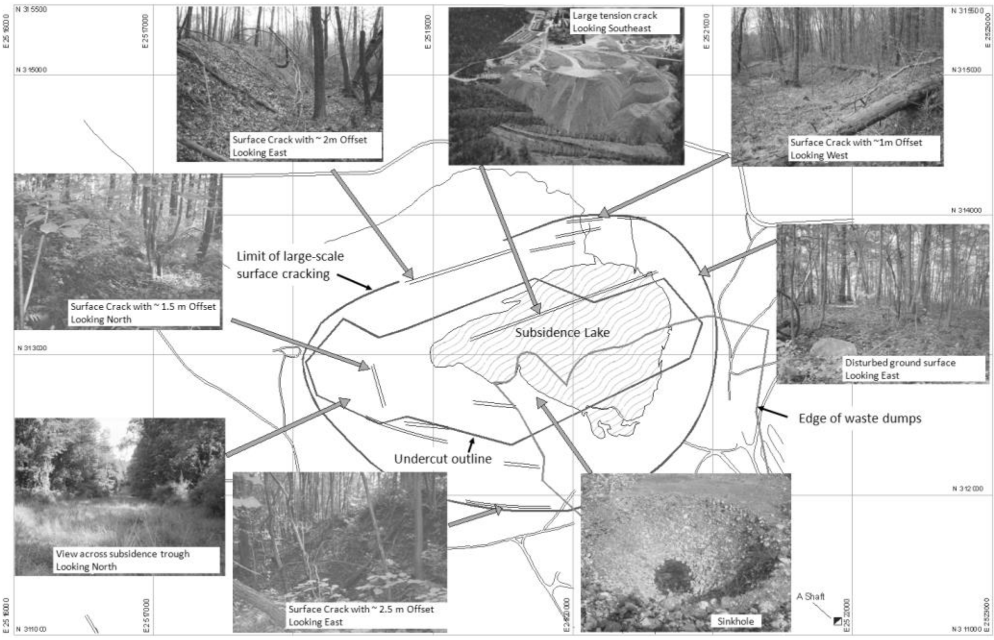

Figure 7 Limit of large-scale surface cracking

In the southwest section of the subsidence trough, a shear-failure mechanism appears to be predominant. Large scarps with offsets of approximately 3 m can be observed. In the northeast section of the subsidence trough, both large tension cracks and shear failure scarps can be observed. In the western section of the subsidence trough, a continuous trough-like basin has formed over the shallower, thinner section of the orebody. A sinkhole that developed after reclamation of the waste dumps can be observed within the limits of the mine workings.

5.3 Conceptual model of subsidence formation at the Grace Mine

Figure 8 illustrates a conceptual model of the caving and subsidence formation at the Grace Mine. In the years after initial breakthrough, the size of the actual crater did not increase significantly, indicating that bulking-controlled caving had prevented the progression of the caved zone to the ground surface. The subsequent subsidence was observed to manifest as a subsidence trough following the direction of mining.

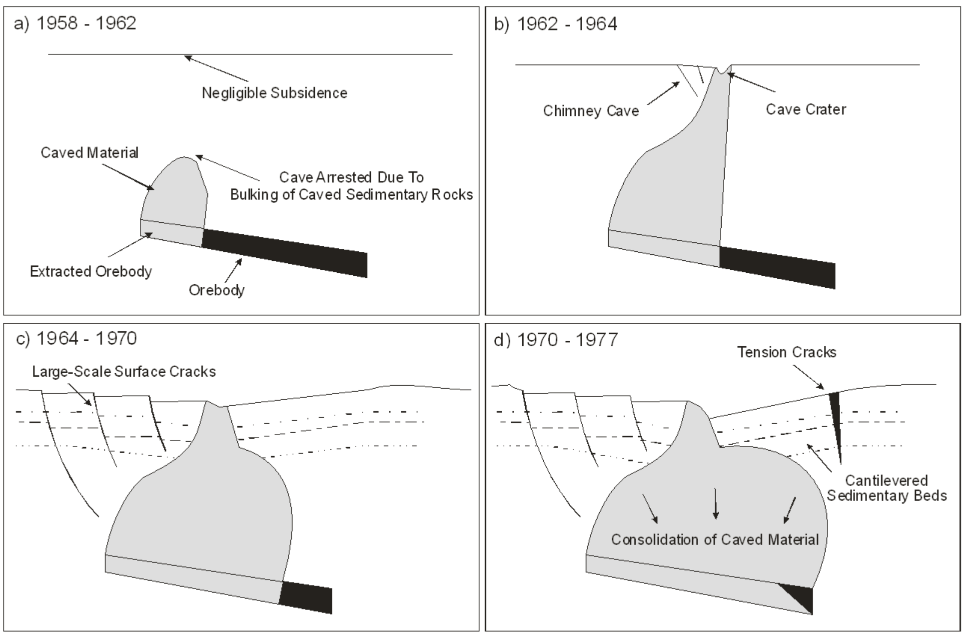

Figure 8 Conceptual model of subsidence formation

The failure mechanism of the ground surface appears to be a combination of shear failure of the side rock, resulting in stepped benches and scarps, and tensile failure caused by cantilevering of the bedded sedimentary rocks.

6 Numerical modelling of cave-induced subsidence

Numerical modelling has been conducted in order to determine the limits of the small-displacements zone (continuous subsidence zone) and the onset of the stable zone surrounding the subsidence trough. The three-dimensional finite difference code FLAC3D (Itasca Consulting Group, Inc., 2009) was used to simulate the actual surface topography, mining geometry and production history of the Grace Mine. Figure 9(a) illustrates the regional model geometry, while Figure 9(b) illustrates the reconstructed undercut geometry used to represent the historical production schedule.

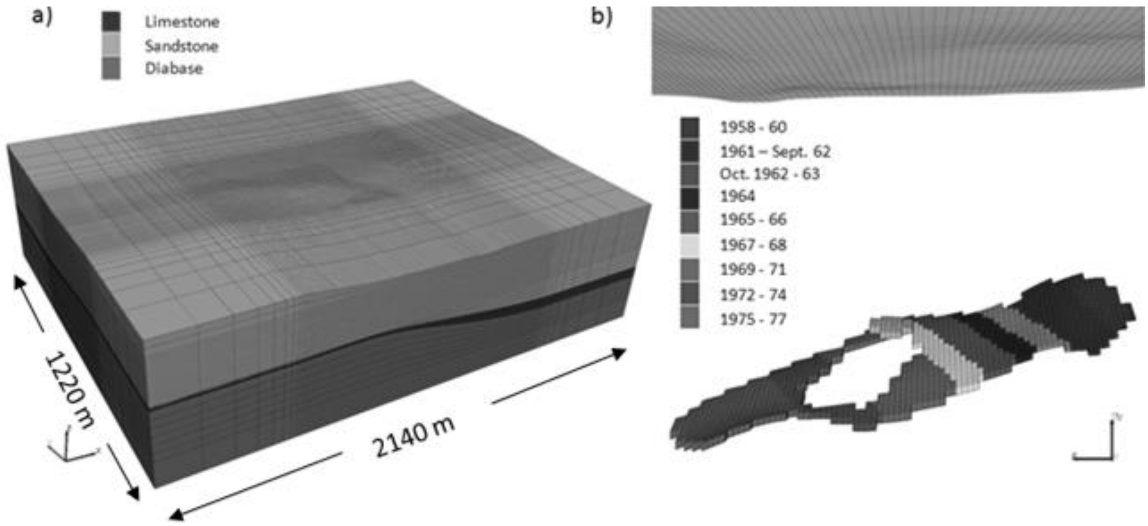

Figure 9 a) Regional extents of model; b) simulated undercut footprint

6.1 Modelling methodology

A numerical approach to modelling of caving has been developed over the past 12 years as part of the industry funded International Caving Study (ICS I and II) and Mass Mining Technology (MMT) projects. The numerical approach is discussed in detail by Sainsbury et al. (2008) and Board and Pierce (2009).

The algorithm is used to represent the primary mechanisms of undercutting, draw and cave propagation. By implementing a bi-linear, Mohr−Coulomb, strain-softening constitutive model to simulate the progressive disintegration of a jointed rock mass to a caved material; together with a production draw technique that accurately accounts for the mass balance of a dilating (bulking) rock mass, the cave is allowed to evolve progressively upward from the undercut.

In order to simulate the mass based production schedule at Grace Mine, recovered from actual hoist records (Table 3), production simulation within the numerical caving model has been controlled by mass balance calculations that are performed at regular intervals during model stepping. Production draw was ceased after the required mass was removed from the system for any given mining period.

Bi-linear Mohr–Coulomb material properties were derived from a least-squares best fit to the Hoek–Brown failure envelope for each rock type using the GSI, UCS and m_i values presented in Table 1.

Table 3 Grace Mine ore production (after Eben, 2004, written comm.)

	1958–1960	1961–September 1962	October 1962–1963	1964	1965–1966
Million tonnes	1.18	2.89	2.35	2.23	4.04

	1967–1968	1969–1971	1972–1974	1975–1977
Million tonnes	3.65	5.74	5.74	4.82

6.2 Predicted evolution of cave mobilised and yield zones

The evolution of the cave mobilised and yield zones above the undercut footprint is illustrated in Figure 10. The mobilised zone (yellow surface) consists of rock blocks that have detached from the rock mass and are moving toward the drawpoints in response to draw. Although the specific location of the caved back is difficult to predict precisely, it is estimated in the numerical model to be defined by zones that have experienced a displacement greater than or equal to 1–2 m. The yield zone (blue surface) represents the region surrounding the cave that is fractured, lost some or all of its cohesive strength and provides minimal support to the overlying rock mass. The yield zone within the numerical model has been defined by zones (elements) that have failed and degraded to zero cohesion or zero tensile strength.

The predicted cave behaviour provides a close match with the reported evolution of cave breakthrough and subsidence trough formation. The yield zone is predicted to intersect the ground surface during 1962 (Figure 10(b)), while the mobilised zone is predicted to intersect the ground surface towards the end of 1963 (Figure 10(c)). This coincides with the first indication of subsidence reported on 10 December 1962 and the breakthrough of the caved (mobilised zone) on 16 December 1963.

As production progresses to the thinner and deeper extents of the orebody (to the east), the predicted mobilised zone does not reach the ground surface (Figure 10(f)). This coincides with the formation of a subsidence trough, rather than an extention of the subsidence crater over the northeast region of the orebody.

6.3 Model validation

The predicted vertical displacement was monitored within the model at the same locations as the USBM subsidence monitoring monuments that were documented by Goodman (1970). The measured versus predicted vertical displacement at three survey monuments surrounding the subsidence trough are illustrated in Figure 11. The predicted surface displacements provide a close match to the monitoring results and provide good confidence in the predicted surface displacements beyond 1969.

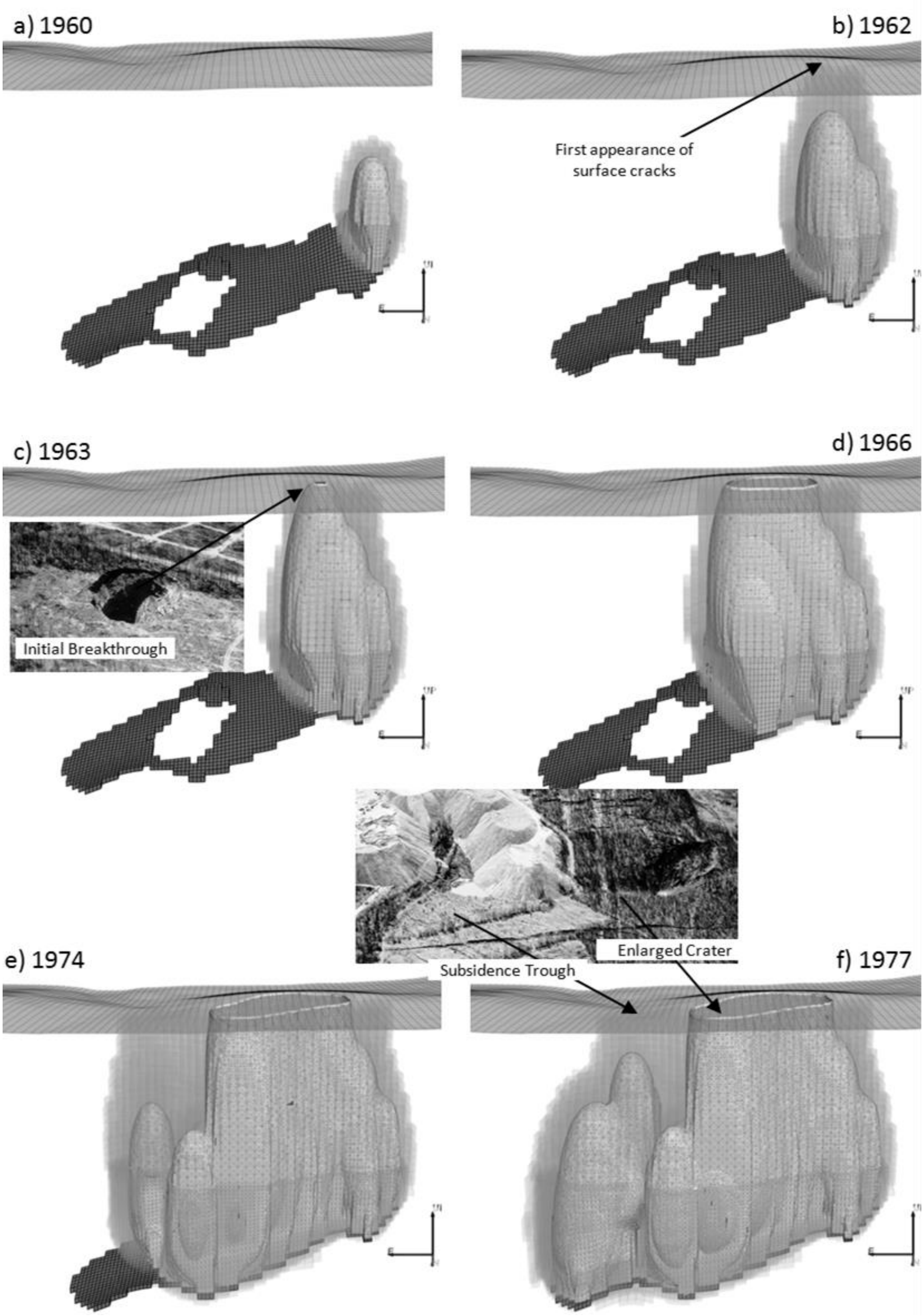

Figure 10 Predicted evolution of cave mobilised and yield zones (looking south)

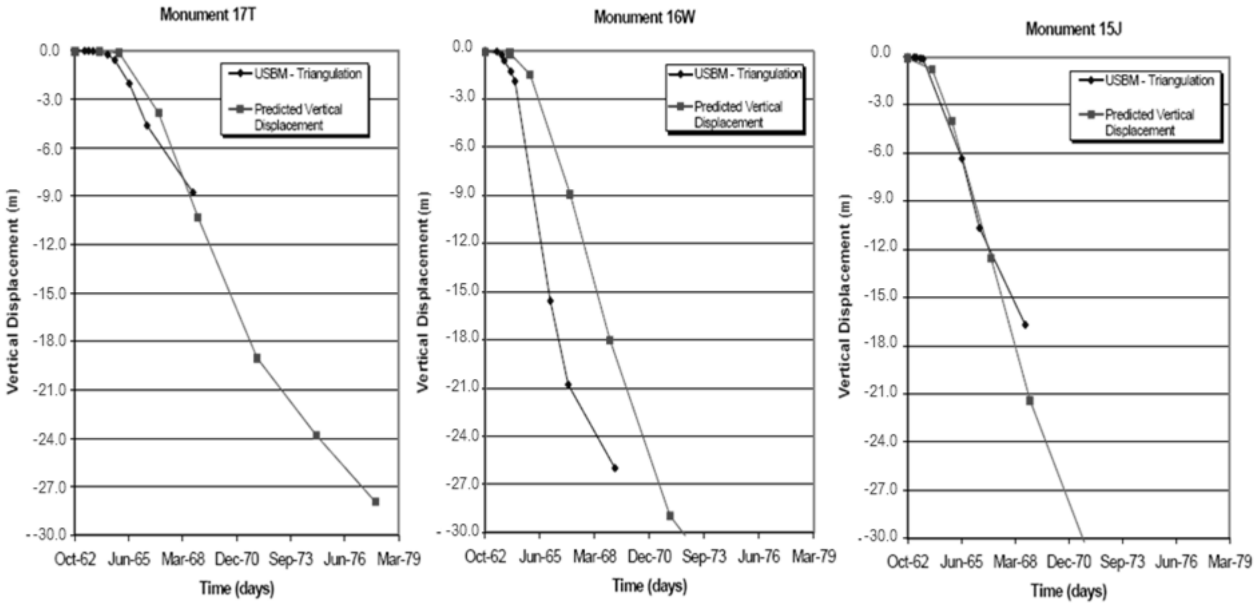

Figure 11 Measured versus predicted vertical displacements from numerical model

6.4 Assessment of the subsidence zone of influence

The limit of small displacements was derived by generating a contour line that encompasses all areas of horizontal strain > 0.002 (0.2%) and angular distortion > 0.003 (0.3%) as illustrated in Figure 12. These strain criteria are based on the surface subsidence required to cause damage to a masonry structure during active subsidence (Singh, 2003).

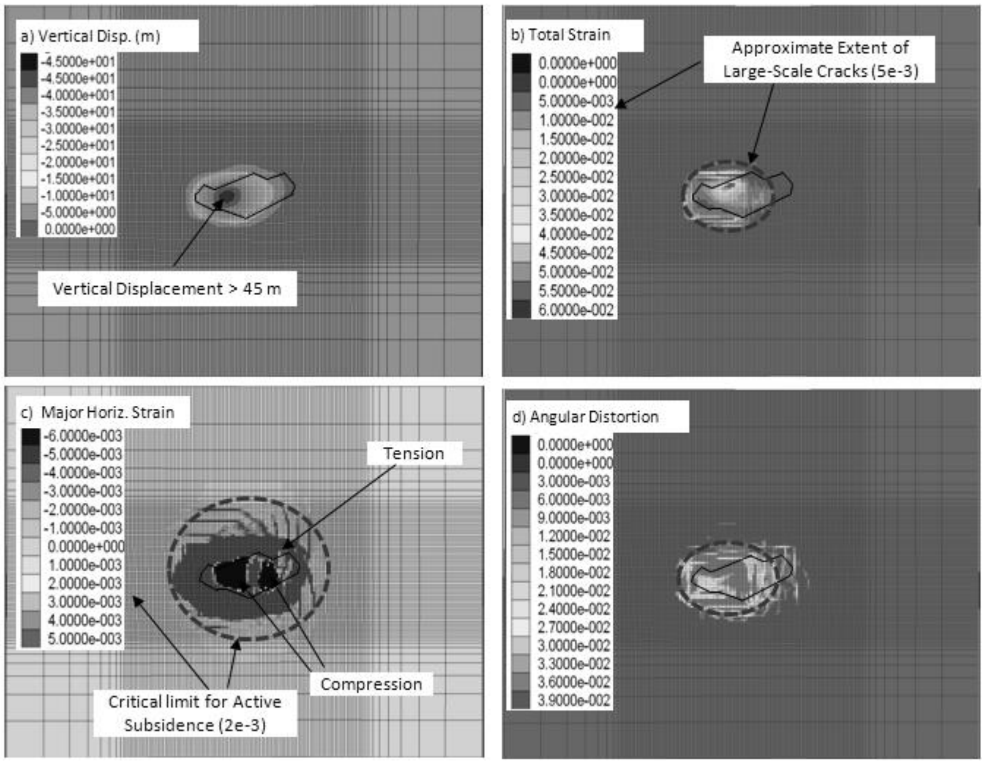

Figure 12 Plan view of a) vertical displacement; b) total strain; c) major horizontal strain; and d) angular distortion

A total strain criterion of 0.005 (0.5%) from the numerical modelling results was also used to confirm the limit of the large-scale surface cracks (Figure 12(b)). This total strain criteria has been used to calibrate the limit of large-scale fracturing at the El Teniente block cave mine in Chile (Cavieres et al., 2003), and provides a close match to the limit of large-scale surface cracks derived by visual observation of the large-scale subsidence features at Grace Mine.

The resulting subsidence zone of influence is illustrated in Figure 13. Although all active subsidence at Grace Mine has ceased, a horizontal strain criteria of 0.002 (0.2%), obtained from the numerical modelling results, was used to define the limit of small displacements that occurred during the active subsidence phase.

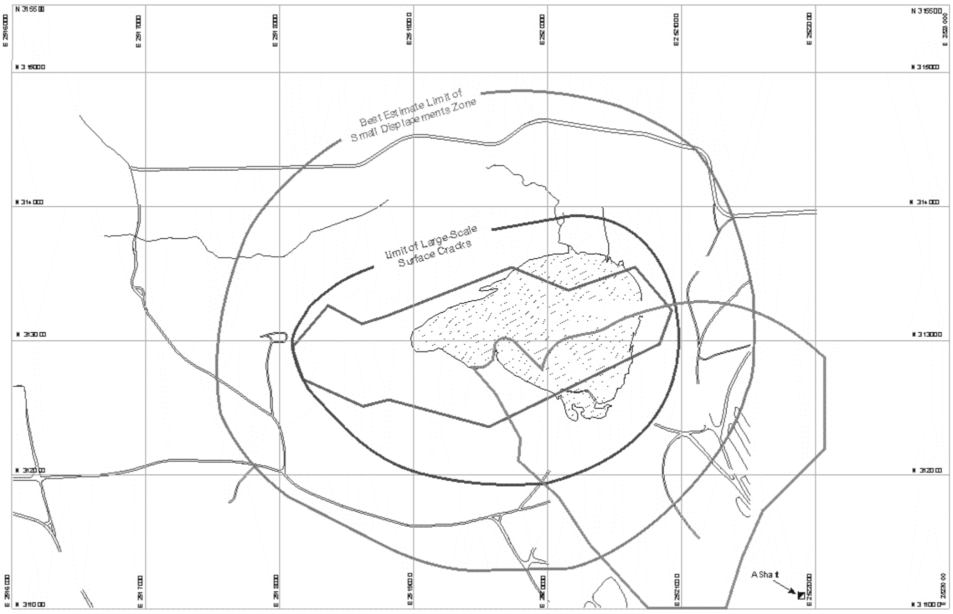

Figure 13 Subsidence zone of influence

7 Assessment of long-term time-dependent subsidence

The time associated with subsidence resulting from mining is composed of two distinct phases: 1) active; and 2) residual. Active subsidence refers to all movements occurring simultaneously with the mining operations, while residual subsidence is that part of the surface deformation that occurs after the cessation of mining.

7.1 Residual subsidence

7.1.1 Mechanisms of residual subsidence

Almost all of the limited research conducted on residual mining-induced subsidence is associated with underground coal mining methods. The duration of reported residual subsidence movements above longwall coal mines is relatively short, typically varying between a few weeks to five years. Singh (2003) reports that the magnitude of residual subsidence displacements rarely exceeds about 10% of the total subsidence. Residual subsidence time spans reported in literature are summarised in Table 4. The duration of mine waste rock fill settlement reported by Williams (2000) is consistent with the duration of residual subsidence reported throughout the literature, as illustrated in Figure 14.

Table 4 Residual subsidence duration over longwall mines (after Singh, 2003)

Reference	Country	Residual Subsidence Duration
Anon (1947)	UK	2–10 years
Collins (1977)	UK	2–4.5 years
Grard (1969)	France	6–12 months
Brauner (1973)	Germany	1–2 years
Brauner (1973)	USSR	4–5 years (deep mines)
Shadrin and Zomotin (1977)	USSR	0.2–2 years
Gray et al. (1977)	US	0.3–3 years
Hood et al. (1981)	US	1 year

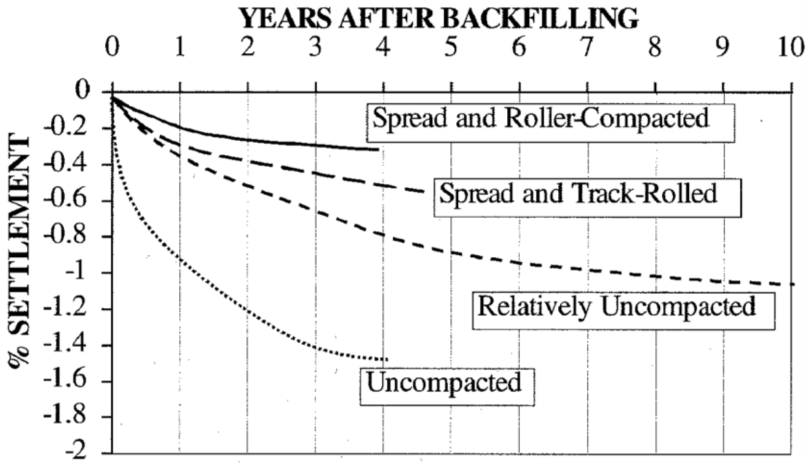

Figure 14 Mine waste rock backfill settlement versus time (Williams, 2000)

Luo and Peng (2000) suggest that the main cause of residual subsidence for longwall coal-mining operations is the recompaction in the overburden strata that was disturbed during the active subsidence process; while Stewart et al. (1984) postulate that the continued crater expansion at the Henderson Mine between 1982 and 1983 was also caused by recompaction of caved material.

As discussed, damage to surface structures is caused mainly by tilt, angular distortion, bending and horizontal strains of the ground surface during the active subsidence phase. Luo and Peng (2000) suggest that residual subsidence manifests in very minor uniform vertical subsidence that, alone, does not cause any structural damage to buildings.

7.1.2 Residual subsidence monitoring

A residual subsidence monitoring network, consisting of 70 monuments, was installed during early 1994 as part of a permit application for an adjacent landfill. Figure 15 illustrates the subsidence-monitoring network located primarily over the western section of the subsidence trough. The elevation change of each monument along the Beta North Line from early 1994 to mid 2003 is shown in Figure 16. There is no trend evident in the survey result that indicates any residual subsidence. All elevation changes recorded are within the inherent error of the survey instruments and methods employed. However, the results do display an increase in error with increasing slope distance (distance from base station to monument).

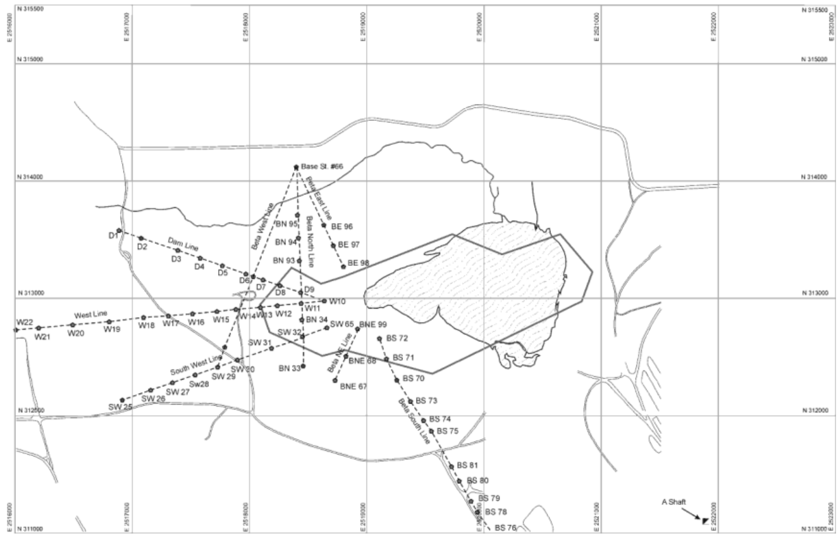

Figure 15 Subsidence monitoring network

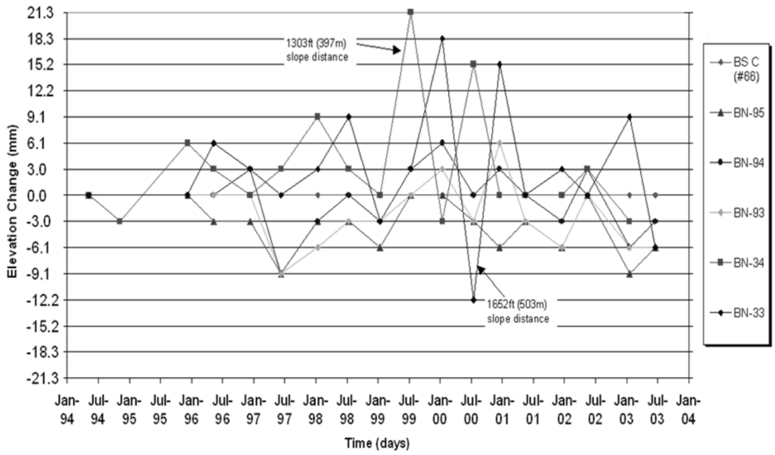

Figure 16 Elevation change along Beta North Line

From the survey results, it is apparent that all residual subsidence in the western section of the subsidence trough has diminished to below levels measurable with current survey techniques within the 17 year period between the cessation of mining in 1977 and commencement to residual subsidence monitoring in 1994.

7.2 Sub-surface erosion

7.2.1 Mechanisms of sub-surface erosion

Several years, or even decades, after mining-induced subsidence stabilised, pot holes have been observed on the surface, mainly around the perimeter of the subsided area where tension cracks existed at the time of subsidence. Coincident with subsidence, deep-seated tension cracks develop in the rock and the overlying soils on the surface. van der Merve (1999) suggests that, due to surface erosion, the cracks within the soil are filled with loose soil and become healed, but the deep-seated cracks within the bedrock remain open and become natural water features for percolating surface water. As water percolates through the soil into the cracks, the surface soils are eroded and form a cavity that eventually breaks through to the surface, as illustrated in Figure 17(a).

The time of development of sub-surface erosion cannot be predicted reliably. However, van der Merve (1999) reports that it is conceivable that the mechanism may take decades or even centuries to develop fully.

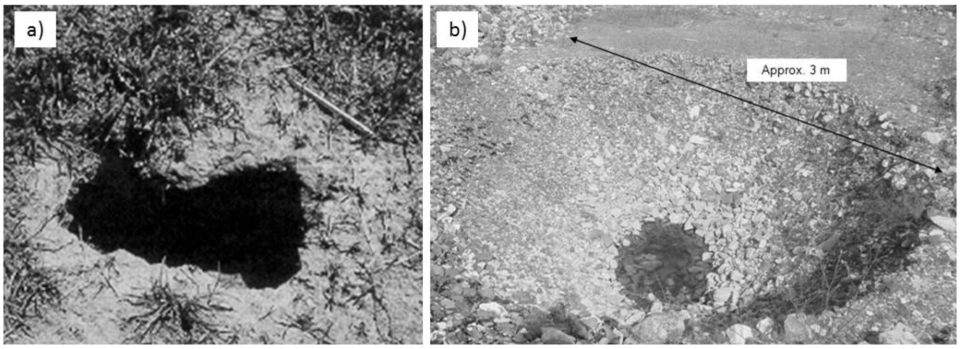

Figure 17 a) Subsurface erosion pot holes (after van der Merve, 1999); b) Sinkhole located within the limit of large-scale cracking

7.2.2 Observation of sub-surface erosion

A sinkhole was observed within the limit of large-scale surface cracking, as illustrated in Figure 17(b). The exact cause of the sinkhole is unknown. It is located in an area of the waste dump that was reclaimed after 1997. This suggests that the sinkhole is associated with a sub-surface erosion mechanism, but it is not clear whether the sinkhole was formed by either sub-surface erosion of deep-seated tension cracks within the underlying disturbed rock mass or sub-surface erosion of unconsolidated waste-rock material.

8 Conclusions

Prior to redevelopment of the abandoned Grace Mine site for residential and light industrial usage, investigation of the subsidence zone of influence, and the potential for further subsidence has been undertaken. The limit of large-scale surface cracking and limit of small-scale displacements has been defined through a combination of field mapping and numerical modelling.

Investigation of residual subsidence (subsidence occurring after mining has stopped) indicates that the subsidence affected rock masses have reached a stable state and ceased subsiding. However, there is limited direct evidence of the post-subsidence phenomenon of sub-surface erosion. This mechanism generally results in small sinkholes and potholes that can develop many years after mining. Due to the highly fractured nature of the rock mass within the limit of large-scale surface cracking, any building, roads, bridges, pipelines or other infrastructure will be subject to the affects of residual subsidence. This area is suitable for the development of parkland or a golf course, although care should be taken to landscape the area with respect to the natural surface watercourses that have been created by the deep-seated subsidence features.

Although no residual subsidence has been monitored with surveying techniques since 1994, the rock mass between the limit of small displacements and the limit of large-scale surface cracks has been disturbed by the panel caving process, and has the potential to undergo residual mining-induced subsidence. Due to the nature of ground disturbance caused by the panel caving mining method, any future mining-induced subsidence will most likely manifest as small-scale surface displacements caused by recompaction of caved material and not the catastrophic and violent development of large sinkholes that are associated with mining induced subsidence in abandoned room-and-pillar coal mining areas such as western Pennsylvanian and Loraine Iron Ore District of France. The area outside the limit of small displacements zone is not expected to be subject to any affects of caving-induced subsidence.

Acknowledgements

Mr Greg Berman from Arcadia Land Company is acknowledged for permission to publish this paper.

References

Agarwal, R., Eben, C.F. and Taylor, C.E. (1973) Rock Mechanics Program at Grace Mine, Technical Report No. 3, Henry Krumb School of Mines, Columbia University, New York.

Anon (1947) Report of the Special Committee on Mining Subsidence, Institution of Municipal Engineers, London.

Basu, D. (1974) Genesis of the Grace Mine Magnetite Deposit, Morgantown, Berks County, Southeastern Pennsylvania, Ph.D. Thesis, Lehigh University.

Board, M. and Pierce, M. (2009) A review of recent experience in modelling of caving, International Workshop on Numerical Modelling for Underground Mine Excavation Design, June 28, Asheville, North Carolina, In conjunction with the 43rd U.S. Rock Mechanics Symposium.

Brauner, G. (1973) Subsidence Due to Underground Mining, U.S. Bureau of Mines, IC 8571.

Cavieres, P., Gaete, S., Lorig, L. and Gomez, P. (2003) Three-Dimensional Analysis of Fracturing Limits Induced by Large Scale Underground Mining at El Teniente Mine, in Soil and Rock America 2003, in Proceedings 39th U.S. Rock Mechanics Symposium, P.J. Culligan, H.H. Einstein and A.J. Whittle (eds), June 2003, Cambridge, Massachusetts, Verlag Glückauf, Essen, pp. 893–900.

Collins, P.J. (1977) Measurement and Analysis of Residual Mining Subsidence Movements, Large Ground Movements and Structures, in Proceedings Conference at University of Wales, Institute of Science and Technology, Cardiff, Wales, Wiley and Sons, New York.

Goodman, T. (1970) Internal USBM monthly subsidence monitoring report.

Grard, C. (1969) Mining Subsidence and the Means Permitting the Limiting of their Effects on the Surface (in French), Revue de l'Industrie Mineral, 51, (January).

Gray, R.E., Bruhn, R.W. and Turka, R.J. (1977) Study and Analysis of Surface Subsidence Over Mined Pittsburgh Coalbed, U.S. Bureau of Mines, J0366047.

Hood, M., Ewy, R.T. and Riddle, L.R. (1981) Empirical Methods of Subsidence Prediction — A Case Study, Workshop on Surface Subsidence Due to Underground Mining, West Virginia University, Morgantown.

Itasca Consulting Group, Inc. (2009) FLAC3D – Fast Lagrangian Analysis of Continua in 3 Dimensions, Ver. 4.0, User's Manual, Minneapolis, Itasca.

Luo, Y. and Peng, S.S. (2000) Long-Term Subsidence Associated with Longwall Mining — Its Causes, Development and Magnitude, Mining Engineering, Vol. 52(10), October.

Lupo, J.F. (1999) Large-scale surface disturbances resulting from underground mass mining, International Journal of Rock Mechanics and Minining Sciences, Vol. 35(4–5), Paper No. 25.

Panek, L.A. (1984) Subsidence in Undercut-Cave Operations, Subsidence Resulting from Limited Extraction of Two Neighboring-Cave Operations, Department of Mining Engineering, Michigan Technological University, Houghton, Michigan.

Sainsbury, B., Pierce, M. and Mas Ivars, D. (2008) Analysis of Caving Behaviour Using a Synthetic Rock Mass (SRM) - Ubiquitous Joint Rock Mass (UJRM) Modelling Technique, in Proceedings 1st Southern Hemisphere International Rock Mechanics Symposium, (SHIRMS), Y. Potvin, J. Carter, A. Dyskin and R. Jeffrey (eds), 16–19 September 2009, Perth, Australia, Australian Centre for Geomechanics, Perth, Vol. 1 – Mining and Civil, pp. 243–253.

Shadrin, A.G. and Zomotin, V.B. (1977) Calculating the Durations of Surface Movements (in Russian), Fiziko-Tekhnicheskie Problemy Razrabotki Poleznykh Isopaemykh, No. 6.

Sims, S.J. (1968) The Grace Mine Magnetite Deposit, Berks County, Pennsylvania, in Ore Deposits of the United States, The Graton-Sales Volume, J.D. Ridge (ed), AIME, New York, Vol. 1, pp. 108–124.

Singh, M.M. (2003) Mine Subsidence, in SME Mining Engineering Handbook (3rd ed), Society for Mining Metallurgy and Exploration, Inc., Littleton.

Stafford, B. (2002) The Grace Mine Story, The Bee Line, Vol. 24, No. 3 and 4.

Stewart, D., Rein, R. and Firewick, D. (1984) Surface Subsidence at the Henderson Mine, in Geomechanics Applications in Underground Hardrock Mining, SME/AIME, New York.

van der Merve, N.J. (1999) Sub Surface Erosion — A Post Subsidence Phenomenon, in Proceedings 9th ISRM Congress on Rock Mechanics, Paris, Balkema, Rotterdam, Vol. 1.

Williams, D.J. (2000) Assessment of Embankment Parameters, Slope Stability in Surface Mining, Littleton, Colorado, SME.